PCCP

Accepted Manuscript

This is an *Accepted Manuscript*, which has been through the Royal Society of Chemistry peer review process and has been accepted for publication.

Accepted Manuscripts are published online shortly after acceptance, before technical editing, formatting and proof reading. Using this free service, authors can make their results available to the community, in citable form, before we publish the edited article. We will replace this *Accepted Manuscript* with the edited and formatted *Advance Article* as soon as it is available.

You can find more information about *Accepted Manuscripts* in the Information for Authors.

ROYAL SOCIETY OF CHEMISTRY

www.rsc.org/pccp

Realizing Chemical Codoping in TiO$_2$

Fang Wang,[a,b] Yi-Yang Sun,[c] John B. Hatch,[b] Hui Xing,[b] Xuechen Zhu,[b] Hongwang Zhang,[b] Xiaohong Xu,[a]

Hong Luo,[b] S. Perera,[b] Shengbai Zhang[*c] and Hao Zeng[*b]

[a]*School of Chemistry and Materials Science, Shanxi Normal University, Linfen 041004, China*

[b]*Department of Physics, University at Buffalo SUNY, Buffalo, New York 14260, USA*

[c]*Department of Physics, Applied Physics & Astronomy, Rensselaer Polytechnic Institute, Troy, New York*

12180, USA

We demonstrate experimentally a chemical codoping approach that would simultaneously

narrow the band gap and control the band edge positions of TiO$_2$ semiconductors. It is shown

that a sequential doping scheme with nitrogen (N) leading the way, followed by phosphorous (P),

is crucial for the incorporation of both N and P into the anion sites. Various characterization

techniques confirm the formation of the N-P bonds, and as a consequence of the chemical

codoping, the band gap of the TiO$_2$ is reduced from 3.2 eV to 1.8 eV. The realization of chemical

codoping could be an important step forward in improving the general performance of electronic

and optoelectronic materials and devices.

Introduction

TiO$_2$ is a wide gap semiconductor commonly used for solar energy harvesting applications. However, its band gap is too large for visible light absorption. Earlier efforts for band gap engineering including monodoping of metal[1,2] and non-metal elements,[3-5] passivated codoping,[6] non-compensated codoping,[7] and surface defect engineering,[8-10] have made great progress to broaden its absorption range. For example, TiO$_2$ nanotube arrays (TNTs) with B-F codoping exhibit better photoelectrochemical and photocatalytic properties than those of F-monodoped TNTs due to the narrower bandgap.[11] TiO$_2$ nanowires with C, N and S codoping could not only broaden the light adsorption spectra into the visible region (400–600 nm), but also inhibit the recombination of photo-induced carriers.[12] The concept of passivated codoping is proposed to eliminate partially occupied impurity bands by introducing donor-acceptor pairs that compensate each other in terms of charge neutrality.[6] However, in non-compensated codoping, such charge compensation is not satisfied.[7,13] Moreover, Chen *et al.* found the photoelectrochemical water splitting performance can be significantly promoted in visible light by constructing the single-crystalline, branched nanowires arrays, such as ZnO nanowires/nanodisks arrays and their sensitization with CdS/CdSe quantum dots.[14]

Another essential requirement for using TiO$_2$ in photocatalytic applications is the correct position of the band edge states for carrier extraction. For spontaneous water splitting, the optical gap of TiO$_2$ should straddle the redox potentials of H$_2$O.[15,16] Since the conduction band minimum (CBM) of pristine TiO$_2$ is only slightly higher than the H$^+$/H$_2$ reduction potential while its valence band maximum (VBM) is much lower than the OH$^-$/O$_2$ oxidation potential, the gap narrowing should be achieved by shifting the VBM upwards. The impact of developing a general approach to simultaneously engineer the band gap and band edge alignment of semiconductors is

2

however, not limited to photocatalysis,[17,18] but also for many other applications ranging from optoelectronics,[19] spintronics,[20] and multiferroicity[21] that require carrier extraction or dopant ionization. Recently, it has been proposed theoretically that oxide semiconductors such as TiO_2 can be codoped with a pair of anion dopants that form strong chemical bonds.[22,23] Different from passivated and non-compensated codoping schemes, both dopants could be acceptors in chemical codoping, while they form fully occupied intermediate bands through chemical bonding. This approach termed chemical codoping has several advantages: 1) The strong bonding between dopants significantly reduces the formation energy, so that higher doping concentration may be achieved. 2) The codopants can be so chosen to eliminate half-occupied states serving as recombination centers detrimental to carrier extraction. Chemical codoping, however, is counterintuitive because impurities with the same charge typically repel each other. Therefore, there is a great challenge to realize experimentally chemical codoping in TiO_2.

Herein we demonstrate experimentally the realization of chemical codoping to engineer the band gap and band alignment of TiO_2 semiconductor simultaneously. Realizing chemical codoping is nontrivial. A single precursor containing both anion dopants would not work since the covalent bonding between them would be so strong that it prevents the incorporation of both anions. To overcome this difficulty, a sequential doping strategy was devised to enhance dopant incorporation and the ability to form new bonds. Anatase structured TiO_2 was codoped with nitrogen (N) and phosphorous (P) anions leading to the formation of new chemical bonds, which lowers its band gap from 3.2 eV to 1.8 eV. This value is much lower than that obtained by N (2.64 eV)[24] or P (2.91 eV)[25] monodoping, and rivals the result reported for non-compensated codoping.[7]

Experimental

Chemical synthesis based on hydrolysis followed by hydrothermal treatment was used to produce TiO_2 nanoparticles.[26] Trioctylphosphine (TOP) and urea were chosen as precursors for phosphorus and nitrogen doping.[27,28] The two elements were sequentially doped: TiO_2 doped with N(P) first followed by P(N) doping was labeled as NP-TiO_2 (PN-TiO_2); while samples doped with P(N) only were labeled as P-TiO_2 (N-TiO_2). Briefly, N-TiO_2 was obtained by dissolving titanium tetraisopropoxide in ethanol; urea dissolved in deionized water was then added dropwise to form amorphous TiO_2 nanoparticles. The product was then sealed in an autoclave and heated at 175 °C for 3 h to obtain the anatase structure. To obtain NP-TiO_2, N-TiO_2 was mixed with TOP and heated at the reflux temperature for 12 h. Details of the procedure are provided in Supporting Information. Uniform and nearly spherical TiO_2 particles with sizes of about 1 μm have been obtained (Fig. S1). These particles contain nanosized crystallites ranging from 5 to 10 nm (Fig. S2). Particles spin-coated on glass substrates were used for X-ray photoelectron spectroscopy (XPS) and UV-vis absorption spectra measurements, while those spin-coated on gold coated glass substrates were used for scanning tunneling spectroscopy (STS). The doping concentration and valence states of the dopants were determined by XPS. The optical band gaps were measured by UV-vis absorption spectra and STS was used to map the spatial distribution and obtain the average band gaps. First-principles calculations were based on density functional theory (DFT) using the Heyd-Scuseria-Ernzerh (HSE) of hybrid functional,[29] as implemented in the VASP program.[30] A supercell of 96 atoms (32 Ti and 64 O) was used to model anatase TiO_2. In the case of chemical codoping, two neighboring O atoms were replaced by N and P, respectively. The atomic structures were optimized until the calculated forces on all atoms were smaller than 0.05 eV/Å.

4

Results and Discussion

N and P were chosen as codopants, which according to first-principles calculation could form a strong chemical bond when both substitute for O.[22] Fig. 1a shows the atomic structure of the N-P pair substituting for two O atom and Fig. 1b illustrates the electronic structure and bonding mechanism of the N-P pair. All the spin orbitals of N_O and P_O are involved in the bonding between the N-P pair. After the hybridization, only two fully occupied orbitals are left in the band gap, as shown in the middle part of Fig. 1b, representing the new VBM. Both gap states exhibit anti-bonding character between P $3p$ and N $2p$, as can be seen in Fig. 1c and 1d, and are higher in energy than the occupied states in either monodoping case, resulting in more efficient band gap reduction. The bonding orbitals are pushed down into the valence band and the anti-bonding orbital is pushed up into the conduction band. The electronic structure analysis suggests that the N-P pair forms a triple bond, which is responsible for the significant drop of the formation energy for the P_O defect next to N_O (as discussed below).

While N monodoping has been done extensively, there are few reports of P doped TiO_2.[31,32] We are not aware of work on P anion doping. The difficulty of P anion doping stems from the mismatch between the ionic radii of P (1.06 Å) and O (0.73 Å). In the few reports of (N,P) codoped TiO_2, the P dopants act as cations replacing Ti ions or as interstitials. With P^{5+} substituting Ti^{4+} and N^{3-} substituting O^{2-}, this can be considered as passivated codoping,[6] since P is a single donor and N is a single acceptor.[33,34] Our DFT calculation suggests that even though the band gap can be reduced to ~2.5 eV, the improvement on light absorption is marginal, which is verified by our experimental results. A well-designed doping strategy is therefore essential to ensure N and P incorporated as anions. Our calculation shows that the presence of N can lower the incorporation energy of P in TiO_2 by about 3.4 eV as a result of the formation of N-P bond.

We therefore adopted a sequential doping scheme, where N was doped first, followed by P doping. Such a scheme is also favored considering the doping kinetics. It is known that TiO_2 nanoparticles synthesized by hydrothermal methods are *n*-type due to O vacancies. We suggest that if N is doped substitutionally at the O sites first, they are likely attracted to the vicinities of the O vacancies due to donor-acceptor attractions. This can facilitate the N-P pair formation if P dopants later assume the O vacancy sites.

The valence states and bonding of N, P, O and Ti in undoped and codoped TiO_2 were analyzed by XPS, as shown in Fig. 2. N *1s* and P *2p* peaks emerge upon doping. These peak positions shift according to the various doping schemes. The chemical shifts are consistent with expected oxidation states and chemical bonding of the dopants, as discussed below. In Fig. 2a, an N *1s* peak centered at 399.6 eV is observed for N-TiO_2 with N concentration of 2.4%. When P doping is carried out after N doping to form NP-TiO_2 (N: 1.0%, P: 3.7%), the N *1s* peak position shifts to a slightly lower binding energy of 398.9 eV. The N *1s* binding energies in both samples are lower than that of N-O adsorption (400-406 eV),[35,36] and consistent with reported values in earlier work on N substitutional doping.[37] This clearly shows that N substitutionally dopes the O sites for both N-TiO_2 and NP-TiO_2 samples. A 0.7 eV red shift in the binding energy of NP-TiO_2 compared to that of N-TiO_2 is consistent with the formation of chemical bonding between N and P, which leads to partial electron transfer from P to N.

Evidence of P ions substitutionally doping at the O sites can be obtained by examining the P *2p* XPS peaks. Fig. 2b presents the P *2p* XPS spectra of NP-TiO_2, P-TiO_2, and PN-TiO_2. A peak centered at about 133.3 eV is found for P-TiO_2, which indicates that P exists as P^{5+}.[38,39] The P atoms were probably incorporated as cations and replaced Ti ions, or adsorbed at the surface of the particles as phosphates. For NP-TiO_2, on the other hand, the P *2p* peak occurs at 132.2 eV.

This 1.1 eV red shift in the binding energy of P dopants in NP-TiO$_2$ strongly suggests that the valence of P dopants is lower than that of P-TiO$_2$. Considering that the peak width of 1.8 eV in NP-TiO$_2$ is 0.3 eV broader than that in P-TiO$_2$, and that the doping concentration is 1% N and 3.7% P, it is reasonable that the peak is actually a superposition of two: one from P dopants occupying the O sites, and the other from P^{5+} substituting Ti^{4+} ions. Due to insufficient spectral resolution, a reliable separation of the two peaks is difficult.

To provide further evidence for N-P chemical codoping, a control experiment using identical precursors and synthetic parameters was carried out, where P was doped first followed by N doping. From the XPS results, it is seen that the P $2p$ peak of PN-TiO$_2$ is located at 133.3 eV, identical to that in P-TiO$_2$, suggesting that P exists as P^{5+}. The inability to obtain P anion doping in PN-TiO$_2$ suggests that N dopants play a critical role in P anion doping. Our DFT calculation shows that without the presence of N, the formation energy for a P-on-Ti (P$_{Ti}$) defect is lower than that for a P-on-O (P$_O$) defect over a wide range of O chemical potential. In the presence of N dopants, however, the formation energy of a P$_O$ defect in the neighborhood of a N$_O$ defect can be lowered by 3.4 eV as a result of the new chemical bonding. From these experimental and theoretical investigations, it is concluded that the only possibility for both N and P to be incorporated as anions is for them to form chemical bonds, which is the case in NP-TiO$_2$.

It is expected that the chemical codoping should lead to significant band gap reduction.[22,23] To verify this, the UV-vis spectra of TiO$_2$, N-TiO$_2$, P-TiO$_2$, PN-TiO$_2$, and NP-TiO$_2$ samples are shown in Fig. 3a. While the optical absorption edges of the N-, P-, and NP-doped samples all shift to lower energy than that of the undoped sample, P-doped TiO$_2$ shows only minimal red shift, with an onset wavelength at about 400 nm. The UV-vis spectrum for N-TiO$_2$ shows larger red shift consistent with earlier reports.[3,40] For NP-TiO$_2$, the absorption edge is red shifted from

370 nm to 680 nm, which corresponds to a band gap of ~1.85 eV. NP-TiO$_2$ also demonstrates the strongest absorption in the visible range between 400 and 700 nm. However, the absorption edge of PN-TiO$_2$ appears slightly blue shifted compared with that of undoped TiO$_2$. It is indicated that the synthesis route of P doping followed by N doping cannot contribute to improve the visible light absorption, which is entirely different from the result of NP-TiO$_2$ with N doping first. Fig. 3b shows the calculated imaginary part (ε_2) of the dielectric constant, which determines the optical absorption. It can be seen that ε_2 is significantly increased from that of undoped TiO$_2$ in the visible region. Meanwhile, the change of ε_2 for (N, P) compensated codoping with P on Ti sites is insignificant, which is consistent with the experimental result that PN-TiO$_2$ shows no improvement from pure TiO$_2$ in optical absorption.

The distinct difference between NP-TiO$_2$ and PN-TiO$_2$ suggests that the band gap reduction in NP-TiO$_2$ is a result of the defect levels introduced into the band gap by substitution of N and P at lattice sites, rather than other possible causes such as grain boundaries or disorders.[8] Otherwise, similar improvement in optical absorption should also be observed for PN-TiO$_2$. Because the VBM states are derived predominantly from O $2p$ states, N or P substitution for O mainly modifies the position of VBM. Thus, the band gap reduction in NP-TiO$_2$ is concluded to be a result of up-shift of VBM, which is a unique advantage of the all-anion codoping approach. The only possibility to introduce states near the CBM is P substitution for Ti. Our first-principles calculation, however, suggests that P$_{Ti}$ is a shallow donor and does not introduce any deep electronic levels.

Undisputable gap reduction by N-P chemical codoping is further evidenced by STS. Most of the measured current-voltage (I-V) curves are non-linear, with negligible current at low bias voltages, reflecting the semiconducting nature of the samples. Fig. 4a-d show the typical I-V

8

curves and differential tunneling conductance (dI/dV) spectra, respectively. The latter reflects the local density of states (LDOS) of samples. Both I-V and dI/dV curves for NP-TiO$_2$ are visibly narrower than those for undoped TiO$_2$, suggesting significant gap reduction. Quantitative band gaps of the samples were obtained by cutting the dI/dV curves with a threshold LDOS (2.5% of the peak value) and the difference in the positive and negative bias voltages was taken as the gap value.[7,41] The threshold was so chosen that the most probable gap value is 3.2 eV for undoped TiO$_2$, consistent with reported values.[7] Fig. 4e and 4f shows the band gap mapping for nanoparticle films over an area of 1×1 μm^2, for both pure and NP-TiO$_2$; the gap values are represented by color scales. From the histograms of the gap values shown in Fig. 4g and 4h, it can be seen that the peak gap values have been reduced from ~3.2 eV for undoped TiO$_2$ to 1.8 eV for NP-TiO$_2$, a 40% reduction. This suggests that N-P chemical codoping creates new and accessible electronic states in the energy gap of TiO$_2$, which further confirms UV-vis absorption results and our theoretical predictions. The distribution of gap values for NP-TiO$_2$, with a full-width-at-half-maximum of 1.5 eV is significantly broader than 0.7 eV for undoped TiO$_2$. This may originate from inhomogeneous doping concentration.

Conclusions

In summary, we have developed a sequential doping strategy to realize chemical codoping on anion sites in TiO$_2$ semiconductor. The formation of new chemical bonds between anion dopant pair in TiO$_2$ results in band gap reduction by ~40%. Various characterizations support theoretical finding that chemical codoping simultaneously controls the band gap and band alignment, which could be an important step forward in improving the general performance of electronic and optoelectronic materials and devices. Formation of covalent bonding between dopants in a solid

state material is a novel phenomenon. Its impact goes beyond the band gap engineering of semiconductors and provides a new direction for tuning the electronic structure of solids.

Acknowledgements

Author Information
Corresponding Author
*Email: zhangs9@rpi.edu; haozeng@buffalo.edu.

References

1 W. Y. Choi, A. Termin and R. M. Hoffmann, *J. Phys. Chem.*, 1994, **98**, 13669-13679.

2 A. Fuerte, M. D. Hernández-Alonso, A. J. Maira, A. Martínez-Arias, M. Fernández-García, J. C.Conesa and J. Soria, *Chem. Commun.*, 2001, **24**, 2718-2719.

3 R. Asahi, T. Morikawa, T. Ohwaki, K. Aoki and Y. Taga, *Science*, 2001, **293**, 269-271.

4 S. U. M. Khan, M. Al-Shahry and W. B. Ingler Jr., *Science*, 2002, **297**, 2243-2245.

5 K. Pathakoti, S. Morrow, C. Han, M. Pelaez, X. J. He, D. D. Dionysiou and H. M, Hwang, *Environ. Sci. Technol.*, 2013, **47**, 9988-9996.

6 Y. Q. Gai, J. B. Li, S. S. Li, J. B. Xia and S. H. Wei, *Phys. Rev. Lett.*, 2009, **102**, 036402.

7 W. G. Zhu, X. F. Qiu, V. Iancu, X. Q. Chen, H. Pan, W. Wang, N. M. Dimitrijevic, T. Rajh, H. M. Meyer, III., M. P. Paranthaman, G. M. Stocks, H. H. Weitering, B. H. Gu, G. Eres and Z. Y. Zhang, *Phys. Rev. Lett.*, 2009, **103**, 226401.

8 X. B. Chen, L. Liu, P. Y. Yu and S. S. Mao, *Science*, 2011, **331**, 746-750.

9 H. N. Chen, Z. H. Wei, K. Yan, Y. Bai and S. H. Yang, *J. Phys. Chem. Lett.*, 2014, **5**, 2890-2896.

10 C. Dette, M. A. Perez-Osorio, C. S. Kley, P. Punke, C. E. Patrick, P. Jacobson, F. Giustino, S. J. Jung and K. Kern, *Nano Lett.*, 2014, **14**, 6533-6538.

11 H. Li, J. H. Xing, Z. B. Xia and J. Q Chen, *Electrochimica Acta*, 2014, **139**, 331-336.

12 F. Dong, W. R. Zhao and Z. B. Wu, *Nanotechnology*, 2008, **19**, 365607.

13 J. P. Fan, X. L. Li, Z. Y. Quan and X. H. Xu, *Appl. Phys. Lett.*, 2013, **102**, 102407.

14 H. N. Chen, Z. H. Wei, K. Yan, Y. Bai, Z. L. Zhu, T. Zhang and S. H. Yang, *Small*, 2014, **10**, 4760-4769.

15 S. J. A. Moniz, S. A. Shevlin, D. J. Martin, Z. X. Guo and J. W. Tang, *Energy Environ. Sci.*, 2015, **8**, 731-759.

16 S. U. M. Khan, M. Al-Shahry, W. B. Ingler Jr., *Science*, 2002, **297**, 2243-2245.

17 A. Fujishima and K. Honda, *Nature*, 1972, **238**, 37-38.

18 M. R. Hoffmann, S. T. Martin, W. Y. Choi and D. W. Bahnmann, *Chem. Rev.*, 1995, **95**, 69-96.

19 H. J. Conley, B. Wang, J. I. Ziegler, R. F. Haglund, Jr., S. T. Pantelides and K. I. Bolotin, *Nano Lett.*, 2013, **13**, 3626-3630.

20 Y. F. Li, R. Deng, B. Yao, G. Z. Xing, D. D. Wang and T. Wu, *Appl. Phys. Lett.*, 2010, **97**, 102506.

21 R. F. Berger, C. J. Fennie and J. B. Neaton, *Phys. Rev. Lett.*, 2011, **107**, 146804.

22 P. Wang, Z. R. Liu, F. Lin, G. Zhou, J. Wu, W. H. Duan, B. L. Gu and S. B. Zhang, *Phys. Rev. B*, 2010, **82**, 193103.

23 R. Long and N. J. English, *Chem. Phys. Chem.*, 2011, **12**, 2604-2608.

24 S. Sakthivel and H. Kisch, *Chem. Phys. Chem.*, 2003, **4**, 487-490.

25 H. Natori, K. Kobayashi and M. Takahashi, *J. Oleo. Sci.*, 2009, **58**, 389-394.

26 B. L. Bischoff and M. A. Anderson, *Chem. Mater.*, 1995, **7**, 1772-1778.

27 J. Yuan, M. X. Chen, J. W. Shi and W. F. Shangguan, *Int. J. Hydrogen Energ.*, 2006, **31**, 1326-1331.

28 A. E. Henkes and R. E. Schaak, *Chem. Mater.*, 2007, **19**, 4234-4242.

29 J. Heyd, G. E. Scuseria, and M. Ernzerhof, *J. Chem. Phys.*, 2003, **118**, 8207-8215.

30 G. Kresse and J. Furthmüller, *Comput. Mater. Sci.*, 1996, **6**, 15-50.

31 L. Körösi, S. Papp, I. Bertóti and I. Dékány, *Chem. Mater.*, 2007, **19**, 4811-4819.

32 R. Y. Zheng, L. Lin, J. L. Xie, Y. X. Zhu and Y. C. Xie, *J. Phys. Chem. C*, 2008, **112**, 15502-15509.

33 L. Lin, R. Y. Zheng, J. L. Xie, Y. X. Zhu and Y. C. Xie, *Appl. Catal. B-Enviro.*, 2007, **76**, 196-202.

34 G. S. Shao, F. Y. Wang, T. Z. Ren, Y. P. Liu, and Z. Y. Yuan, *Appl. Catal. B-Enviro.*, 2009, **92**, 61-67.

35 J. Ananpattarachai, P. Kajitvichyanukul and S. Seraphin, *J. Hazard. Mater.*, 2009, **168**, 253-261.

36 J. A. Rodriguez, T. Jirsak, J. Dvorak, S. Sambasivan and D. Fischer, *J. Phys. Chem. B*, 2000, **104**, 319-328.

37 X. B. Chen and C. Burda, *J. Phys. Chem. B*, 2004, **108**, 15446-15449.

38 Handbook of the elements and native oxides, XPS international, Inc. 1999.

39 S. J. Splinter, R. Rofagha, N.S. Mcintyre and U. Erb, *Surf. Interface Anal.*, 1996, **24**, 181-186.

40 M. Sathish, B. Viswanathan, R. P. Viswanath and C. S. Gopinath, *Chem. Mater.*, 2005, **17**, 6349-6353.

41 J. G. Tao, T. Luttrell and M. Batzill, *Nat. Chem.*, 2011, 3, 296-300.

Figure captions:

Fig. 1 (color online). (a) Atomic structure of an N-P pair substituting for two O atoms. (b) A schematic showing the bonding mechanism of the N-P pair. The lower (upper) gray areas represent the valence (conduction) band of undoped TiO_2. (c) and (d) show the charge density isosurfaces of the lower and higher gap states, respectively, of the N-P pair. Both orbitals show an anti-bonding character between P *3p* and N *2p* orbitals. To clearly show the *p-p* anti-bonding, the orientations of atomic structures in (c) and (d) are different from that in (a). An N-P-Ti triangle in pink color has been used to guide the eye.

Fig. 2 (color online). XPS of core level electron peaks of N *1s* and P *2p*. (a) N *1s* peak of NP-TiO_2, N-TiO_2, and PN-TiO_2. (b) P *2p* peak of NP-TiO_2, P-TiO_2, and PN-TiO_2. The dots are raw XPS data and the lines are fittings, respectively.

Fig. 3 (color online). (a) Experimental UV-vis absorption spectra of TiO_2, N-TO_2, P-TiO_2, PN-TiO_2, and NP-TiO_2. (b) Calculated imaginary part (ε_2) of the dielectric constant for undoped TiO_2, N-P chemical codoped TiO_2, where both N and P substitute for O, and (N, P) compensated codoped TiO_2, where N substitutes for O and P substitutes for Ti. The dopant concentration is one N-P pair per 96-atom supercell (i.e., about 1% N and 1% P).

Fig. 4 (color online). Typical I-V curves and dI/dV spectra of undoped TiO_2 (a, c) and NP-TiO_2 (b, d). From representative regions, spatial mapping of the band gaps in an area of 1 μm $\times$1 μm in size (gap values are represented by color scales) and the corresponding histograms of the band gaps for undoped TiO_2 (e, g) and NP-TiO_2 (f, h).
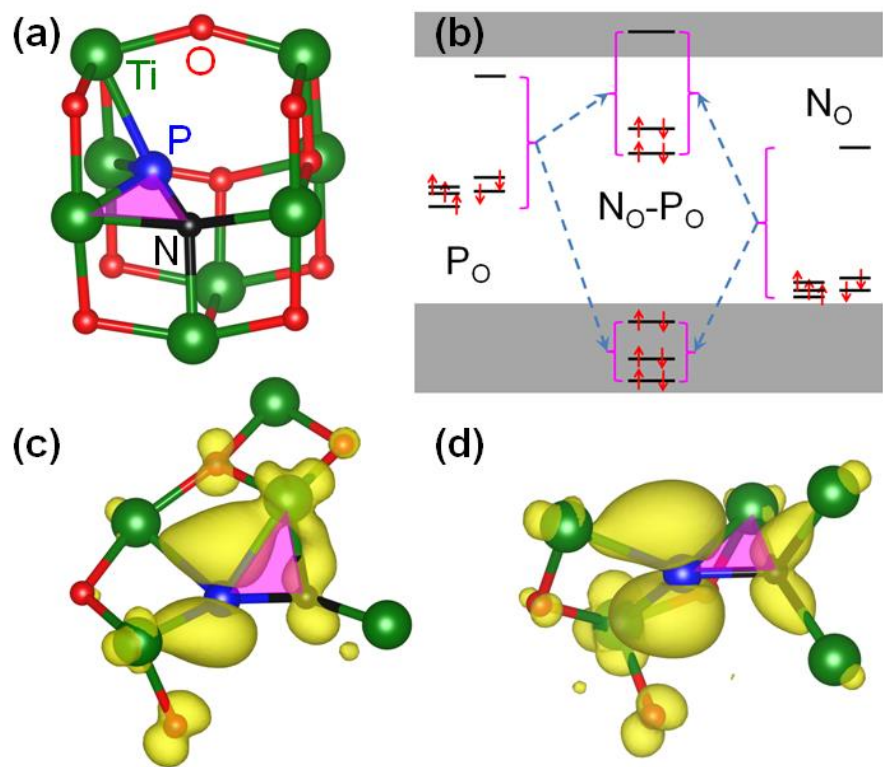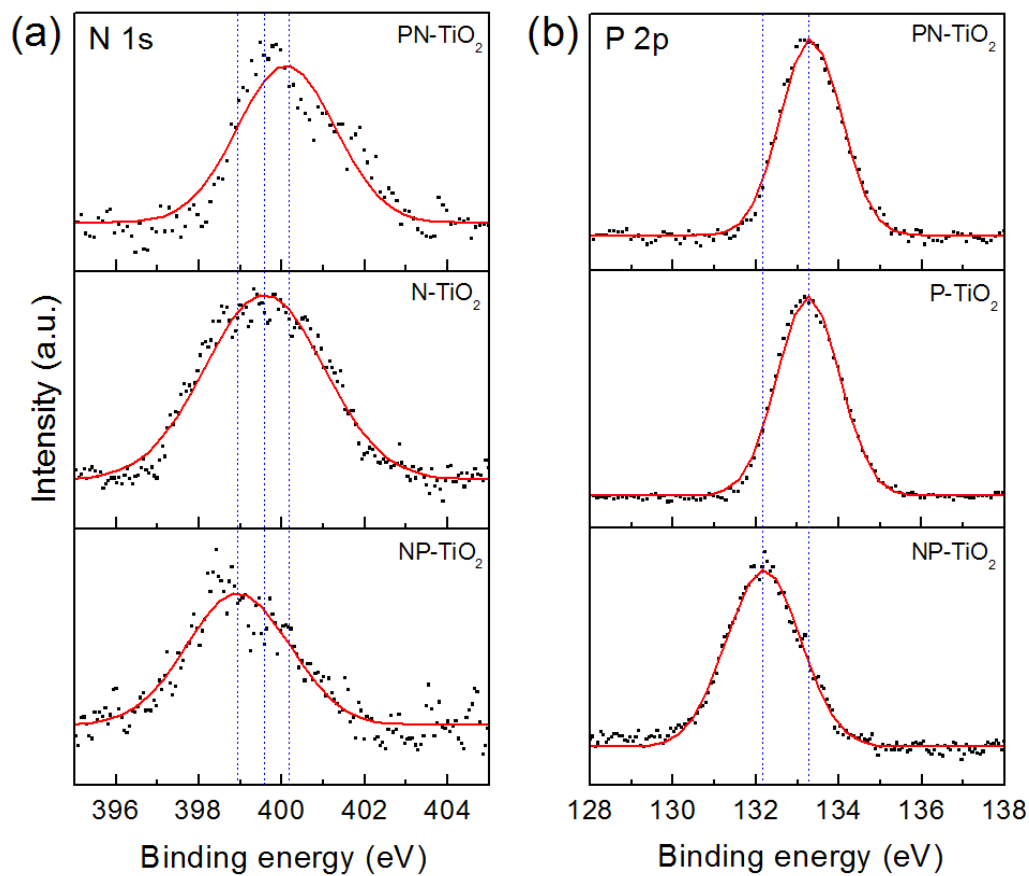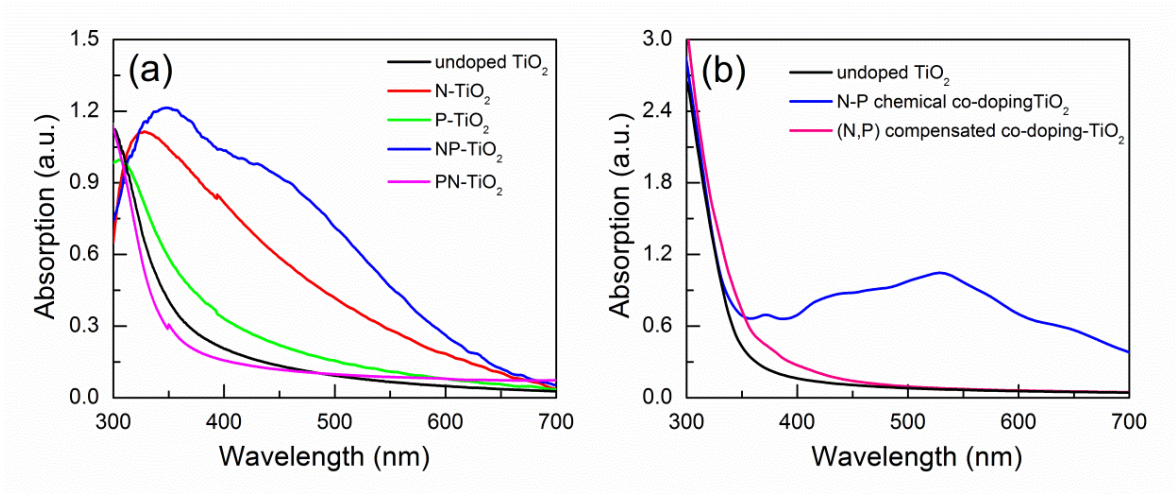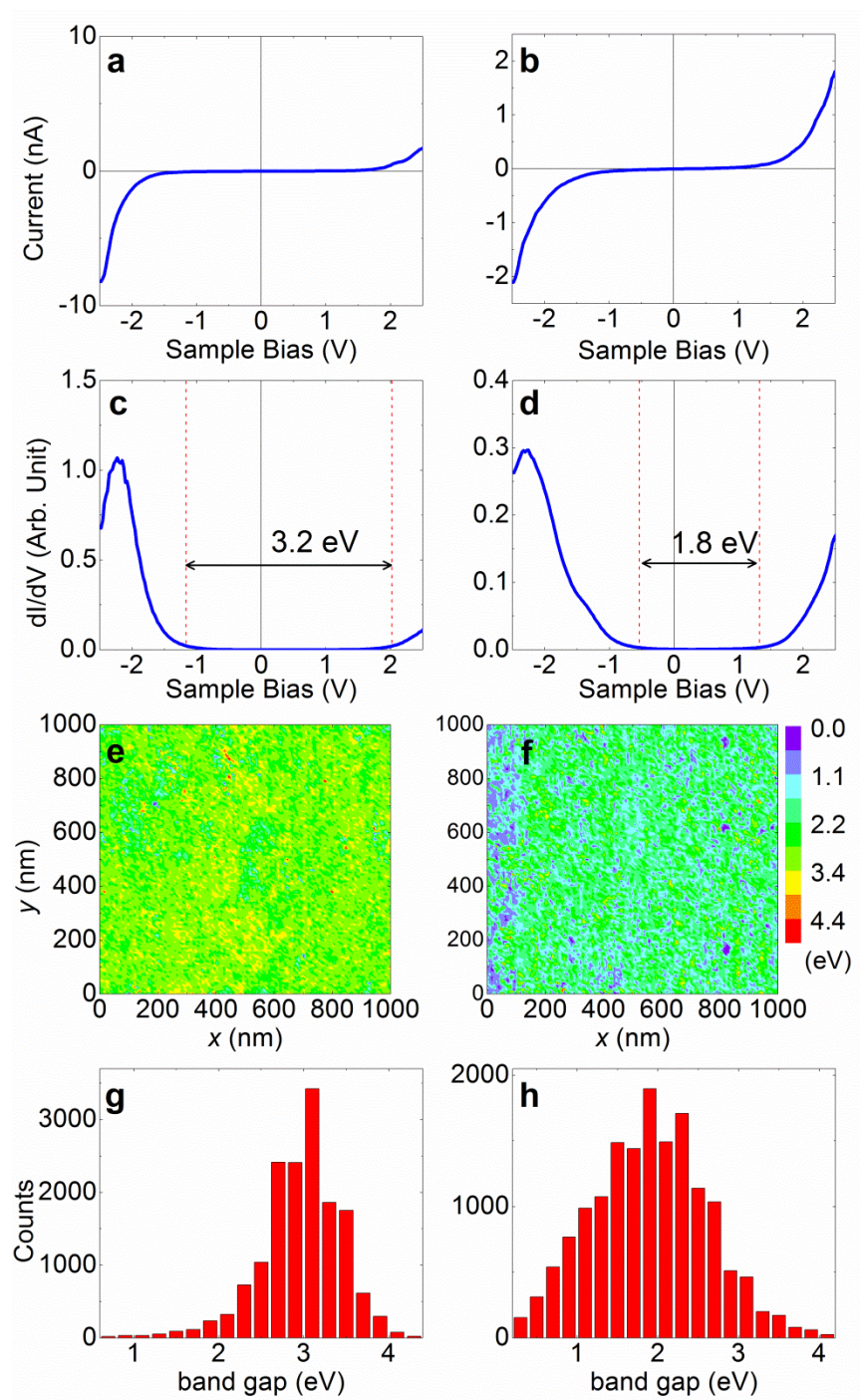
Fig. 1

Fig. 2

Fig. 3

Fig. 4